Geotechnical Aspects of Underground Construction in Soft Ground – Yoo, Park, Kim & Ban (Eds)

Three-dimensional arching effect on vertical circular shafts

S.S. Jeong
Yonsei University, Seoul, South Korea

K.Y. Kim
Korea Electric Power Research Institute, Daejeon, South Korea

H.S. Lim
Yonsei University, Seoul, South Korea

ABSTRACT: The lateral earth pressure of vertical circular shaft is investigated by using experimental test and a numerical analysis. A framework for determining the earth pressure distribution on the basis of both centrifuge model test and 2D FE analysis results is introduced. Through these studies, it is found that the lateral earth pressure acting on a vertical circular shaft considering arching effect is about 80% smaller than that calculated by Rankine's theory. It is also found that arching effect is highly dependent on the shaft diameter, the bearing condition and the flexural modulus of shaft. And it is shown that arching effect of soil is more significant for flexible vertical shaft than for rigid vertical shaft embedded in weathered soil.

1 INTRODUCTION

Arching is the stress distribution process by which stress is transferred around region of soil mass, which then becomes subject to lower stresses (Paik and Salgado, 2003). Much work has been done to study the lateral earth pressure acting on a rigid retaining walls considering arching effect by many researchers. Handy (1983) analyzed soil arching action behind retaining walls, and Wang and Yen (1973) carried out this analysis for slopes. Nakai et al. (1997) performed a series of physical model tests under a 1 g conditions and carried out numerical analysis of these tests to investigate the arching effect. They found that the results obtained from the model tests were in good agreement with those obtained from the numerical analysis. Recently, Janssen (1985) suggested the theoretical basis for the understanding of arching effects in silos. Based on this arching theory, Spangler and Handy (1984), Harrop-Williams (1989) and Wang (2000) suggested equations to estimate the nonlinear distribution of active pressure on retaining walls. Relatively little work has addressed lateral earth pressure distribution acting on the flexible and circular vertical shaft. More recently, Kim et al. (2013) conducted centrifuge model and full-scale field test. They concluded that the lateral earth pressure acting on a circular type of vertical shaft is less than other types of geotechnical structures since three dimensional arching effects (i.e. convex arching and/or inverted arching) are involved. However, no practical solutions are currently available for the determination of lateral earth pressure considering shaft displacements and movements of the surrounding ground. In engineering practice, the displacements are often controlled or limited by choice of a suitable factor of safety and excessive yielding is prevented by an appropriate construction sequence (Wong and Kaiser, 1988).

The objective of this study is to investigate real magnitude and distribution of lateral earth pressure acting on the vertical circular shaft considering the three-dimensional arching effect in weathered soil. Therefore, a series of centrifuge model test and FE analyses for vertical shaft were performed.

2 CENTRIFUGE MODEL TEST

2.1 *Testing apparatus*

A series of centrifuge model tests were performed to investigate the earth pressure distribution of vertical circular shaft in sand. A centrifugal acceleration factor of N = 75 g is used in this study. The geotechnical centrifuge used in this study was located at Daewoo Institute of Construction Technology (DICT). DICT's geotechnical centrifuge was manufactured by Actidyn company in France and corresponds to an Actidyn system C65-2, with a platform radius of 3.0 m and a maximum capacity of 120 g-ton.

Model vertical shaft was made of aluminum alloy with a hollow circular section, 200 mm embedded height, and 80 mm outer diameter (Fig. 1a). It was equivalent to reinforced concrete vertical shaft of height 15 m, and outer diameter 6 m at prototype scale.

(a) Model vertical shaft

(b) Soil sample box

Figure 1. Testing apparatus; (a) Model vertical shaft, (b) Soil sample box.

To investigate the lateral earth pressure at each excavation stage, test model was divided two sections. A small soil sample box 700 × 400 × 200 mm was made with a steel frame (Fig. 1b).

A variety of instrumentations were installed to monitor displacements and earth pressures during the testing. The displacement of vertical shaft wall was measured by two linear variable differential transformers (LVDTs) located on both sides of the shaft surface shown in Fig. 2(a). Pre-calibrated Kyowa earth pressure transducers were installed on the external surface of vertical cylinder wall to measure the lateral earth pressures acting on the vertical shaft, and their locations in the model are also shown in Fig. 2(b).

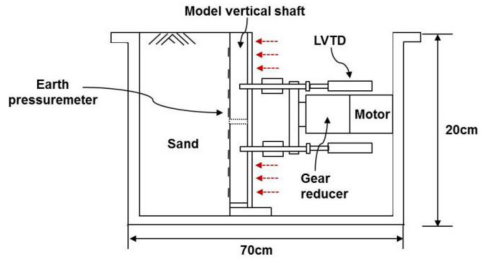

(a) Sectional view

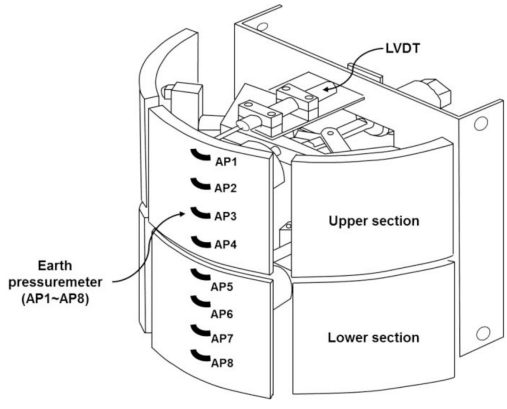

(b) Vertical circular shaft model

Figure 2. Sectional view of the soil sample box and vertical shaft model.

Table 1. Properties of the test soil.

Type	γ (kN/m^3)	ϕ (deg.)	D_r (%)	D_{10} (mm)	C_u	G_s
Silica sand (SP)	12.66	36.95	81∼82	0.091	1.53	2.65

2.2 *Testing program*

Centrifuge model tests were performed on 1/75th scale models for lateral earth pressure acting on the vertical shaft with excavation.

Silica sand classified as SP (according to the Unified Soil Classification System) with a specific gravity (G_s) of 2.65, an effective grain size $D_{10} =$ 0.091 mm and the uniformity coefficient $C_u = 1.53$ was used for centrifuge test. The properties of test soils are summarized in Table 1.

The dry sand sample with a relative density D_r of about 81∼82% (dense state) was prepared by the air pluvial method using an automatic sand-rainer. The spreader was passed repeatedly over a soil sample box until the thickness of the sand layer was approximately 200 mm (15 m on the prototype scale).

After completing sample preparation, the sample box was mounted on the platform of the centrifuge. The lateral earth pressure acting on the vertical shaft was monitored during the excavation. To simulate the excavation step, incremental active wall displacement (δ_h/H, δ_h: horizontal displacement, H: Height of vertical shaft) was chosen to be 1.0 mm/140 sec using a multi-gear motor. Terzaghi (1920) suggested that the active earth pressure occurs at about 0.1%H of active wall displacement. This value is applicable to 15mm wall displacement in this test. The response of lateral earth pressure with excavation was considered by independently controlling divided two sections. First, the diameter on upper section of vertical shaft was gradually reduced to simulate upper excavation, and then earth pressure meters were monitored. Next, the diameter on lower section of vertical shaft was gradually reduced to simulate lower excavation, and then changed earth pressure was monitored.

2.3 *Test results and discussion*

Some typical results from centrifuge model tests are presented here. Fig. 3 shows the results from typical test with measured earth pressure under the condition of active wall displacement. As shown in Fig. 3(a), it is noted that the lateral earth pressure on upper section of the vertical shaft (AP1∼AP4) at first excavation step gradually decreases, until a wall displacement is reached at about 0.2×10^{-2}. This curve demonstrated the reductions in lateral earth pressure with gradual increase of wall displacement. When the active wall displacement (δ_h/H: 0.2×10^{-2}) is occurred, the earth pressure was about 30% (AP4) decreases in initial earth pressure. At this time, the earth pressure on lower section (AP5-AP8) of vertical shaft is measured in a constant. In the second excavation step, where the earth pressure in lower section of the vertical shaft, large reductions of earth pressure are occurred in Fig. 3(b). When the active wall displacement (δ_h/H: 0.2×10^{-2}) is occurred, the earth pressure was about 80% (AP8) decreases of initial earth pressure. Additionally, an earth pressure acting on the upper part (AP1–AP4) of vertical shaft tends to increase as the active displacement of lower part increases. Furthermore, an increase of lateral earth pressure in the active displacement from 0 to 0.2 results in about 10∼30%. Similar magnitude of earth pressure as initial condition (before the first excavation) is measured when the active wall displacement was increased from 0 to 0.6.

Fig. 4 shows a comparison of the test result and Rankine's theory. All the measured data have a relatively smaller earth pressure than the result of the theoretical solution. Based on this, it is verified that the overall lateral earth pressure acting on the vertical circular shaft was reduced approximately 80% compared with the initial condition and theoretical solution. From the test results, it is also found that the lateral earth pressure at deep depth decreased with in active displacement (δ_h/H: 0.2×10^{-2}), beyond which it continue to increase toward the initial condition as

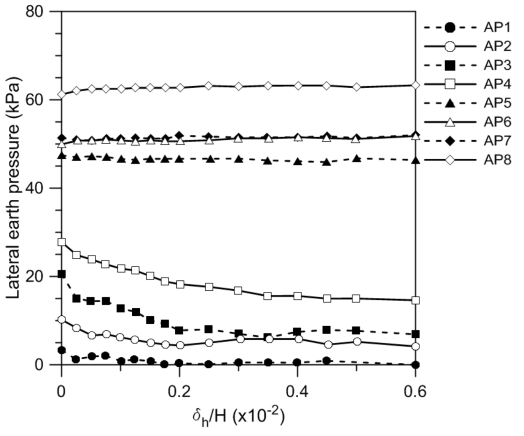

(a) Upper section

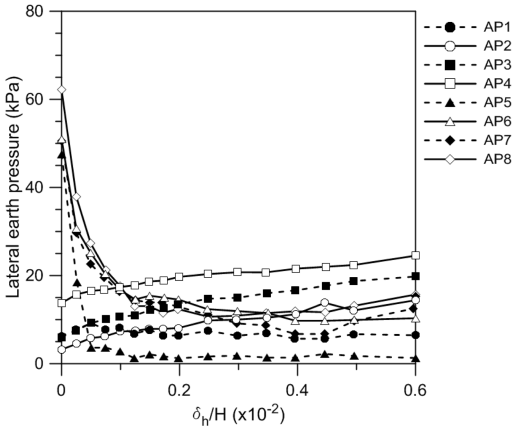

(b) Lower section

Figure 3. Earth pressure distributions: (a) upper section; (b) lower section.

displacement increase. This finding is similar from what Tatiana and Mohamed (2010) discussed about active displacement for a wall. On the other hand, test vertical shaft is excavated into a relatively shallow depth, there is very little reduction of earth pressure. The reason for this behavioral difference between deep and shallow depth is explained by the fact that the weight re-distribution caused by the arching effect will produce more pressure reduction in the deep depth than shallow depth (Kim et al., 2013).

3 NUMERICAL ANALYSES

3.1 *Numerical modeling*

The commercial FE computer program PLAXIS 2D (2012) is used in the numerical analysis. Fig. 5 shows the typical 2D axisymmetric FE model used in this work. The vertical shaft was modeled using five-node plate element. The basic soil elements are 15-node

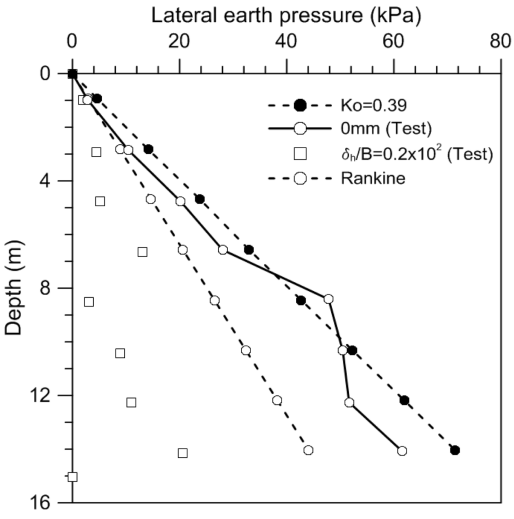

Figure 4. Comparison of earth pressure distributions.

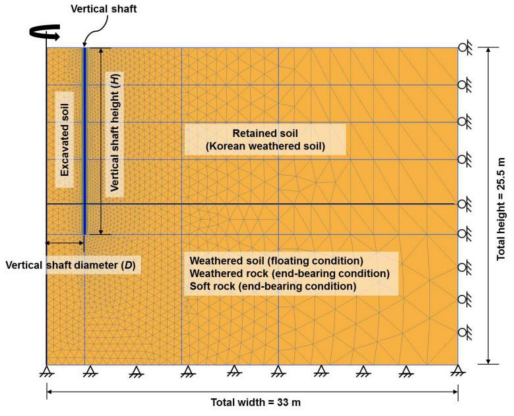

Figure 5. 2D axisymmetric FE model for a vertical shaft (D = 6 m and H = 15 m).

wedge elements which are composed of 6-node triangular elements in horizontal direction and 8-node quadrilaterals in vertical direction.

The overall dimensions of the model boundaries comprise a width of ten times the vertical shaft diameter (D) from the shaft center and a total height equal to the vertical shaft height (H) plus a further 0.7H below shaft toe level. These dimensions were considered adequate to eliminate the influence of boundary effects on the vertical shaft performance. The typical vertical shaft was taken to be 6.0 m in diameter D and 15 m in height H. Here the end-bearing vertical shaft is bearing on weathered rock (or soft rock) through weathered soil layer. The mesh consists of fifteen-node wedge elements, with a total of 39,261 nodes.

Table 2. Summary of material parameters used for validation.

Type	γ (kN/m^3)	E (MPa)	ϕ (deg.)	c (kPa)	ν	Model
Silica sand	12.6	10	36.95	4.50	0.3	M.C
Vertical shaft (Aluminum)	27–	72,000	–	–	0.2	L.E

The vertical boundaries are allowed to displace only in the vertical direction and the bottom boundary is fixed the horizontal and vertical direction, hence assuming a stiff undeformable stratum such as a rock layer. The specified initial stress distributions should match with a calculation based on the self-weight of the material. After the initial step, the soil excavation was simulated by removing soil in lifts. The total soil depth removed was performed in 4 steps for for 15 m vertical shaft, respectively. The vertical shaft was installed when the excavation completed. The vertical shaft is considered as linear-elastic material at all times, while for the surrounding soil layer the Mohr–Coulomb non-associated flow rule is adopted.

3.2 *Validation with centrifuge model test*

In this section, the validation of the numerical modeling techniques is discussed on the basis of the results of FE analysis for the present centrifuge model test. As discussed in section 2, the vertical shaft and soil properties employed for this validation were the same properties mentioned in the centrifuge model test. The material properties of silica sand and vertical shaft are summarized in Table 2. A 2D axisymmetric model was also used and the lateral displacements (δ_h/H: 0.2×10^{-2}) are applied to simulate the excavation procedure, as described in section 2.3.

The representative results of the FE analysis and centrifuge model test are shown in Fig. 6. In these figures, it is clearly found that the present numerical predictions match the experimental measurements quite well for each section of vertical shaft. However, the computed lateral earth pressure near the upper section of vertical shaft is somewhat smaller than the experimental result, because used FE numerical model (i.e. continuum analysis) might not be considered the separation behavior between the vertical shaft and soil compared with the actual phenomenon.

4 PARAMETRIC STUDIES

An extensive parametric study was carried out to investigate the influencing factor of the arching behavior acting on the vertical shaft that could not be specifically identified in the centrifuge model tests. A series of FE analyses on vertical shaft in weathered soil

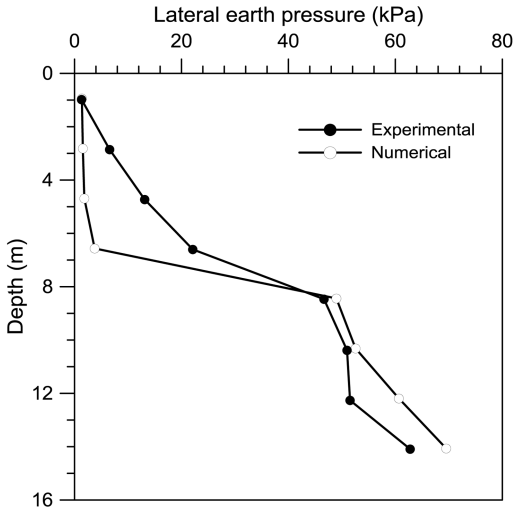

(a) Upper section

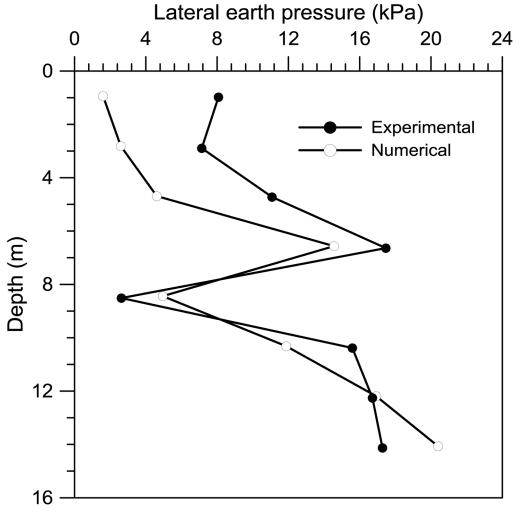

(b) Lower section

Figure 6. Comparison of the results (δ_h/H: 0.2×10^{-2}): (a) Upper section, (b) Lower section.

Table 3. Summary of numerical analyses conducted.

Parameters	Case
Diameter of vertical shaft (D)	D = 3, 6, 9 and 12 m (H = 15 m)
Elastic modulus of vertical shaft (E)	E = 250, 1500, 3000, 5000, 10000 and 28000 MPa (D = 6 m, H = 15 m)
Bearing layer	Weathered soil Weathered rock Soft rock

Table 4. Material properties used in the analyses (parametric studies).

Type	γ (kN/m^3)	E (MPa)	ϕ (deg.)	c (kPa)	ν	Model
Weathered soil	19	50	35	15	0.32	M.C
Weathered rock	21	300	39	34	0.3	
Soft rock	23	500	40	50	0.25	
Vertical shaft	5	250	–	–	0.4	L.E

were performed based on the influencing parameters, such as the shaft diameter (D), the bearing layer and the elastic modulus of shaft (E), as summarized in Table 3. And material properties used in the FE analyses are shown in Table 4.

4.1 *Effect of shaft diameter*

In this section, Fig. 7(a) shows the lateral earth pressure versus the soil depth with varying shaft diameters (D = 3.0, 6.0, 9.0 and 12.0 m) with the same shaft height (H = 15 m). The soil depth was normalized by the shaft height. As shown in the figure, the distribution of the lateral earth pressure is not triangular, which is consistent with Rankine's theory. It is shown that as the shaft diameter increases, the lateral earth pressure in the upper zone of the shaft increases. This is because the variation in the shaft diameter has slight impact on the arching-induced lateral load transfer. It can be explained that the load acting on the shaft increases as the shaft diameter increases, but the arching effect by tangential stress of soil decreases. In other words, when shaft diameter increases, distribution of lateral earth pressure is close to the plane strain condition. This finding is similar to what Liang and Zeng (2002) discuss about the effect of shape in drilled shaft.

Fig. 7(b) shows the final shaft deformed shapes at the end of excavation. The deformed shape is shown that most of the shaft move away from the soil toward the excavation through the height of the shaft, indicating active conditions behind the shaft. With an increase in the lateral earth pressure, deformation of shaft gradually is increased.

4.2 *Effect of bearing layer*

In order to investigate the effect of bearing layer, additional FE analyses are conducted under the multi-layered soil condition. Here the vertical shaft is embedded in weathered or soft rocks through weathered soil varying thicknesses ranging up to 15 m. The comparison results according to end bearing condition are shown in Fig. 8. As expected, the results

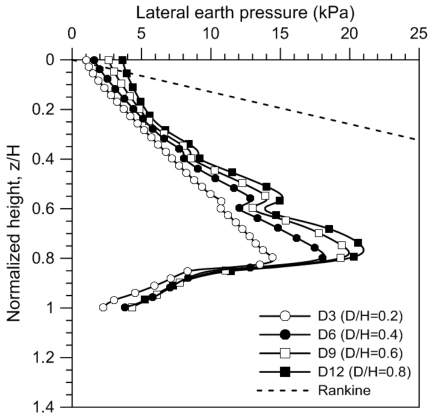

(a) Lateral earth pressure distribution

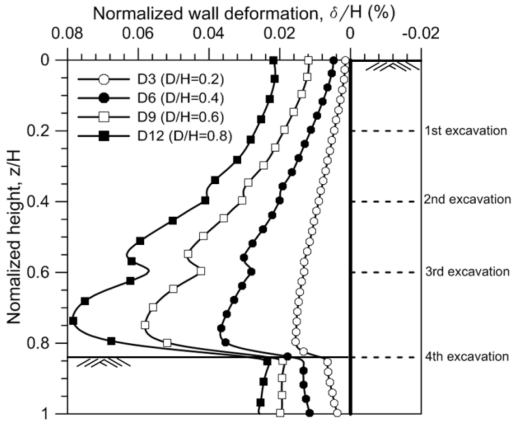

(b) Shaft deformation

Figure 7. Effect of shaft diameter: (a) Lateral earth pressure distribution, (b) Shaft deformation.

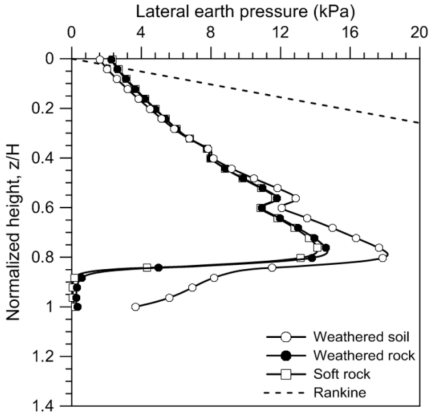

(a) Lateral earth pressure distribution

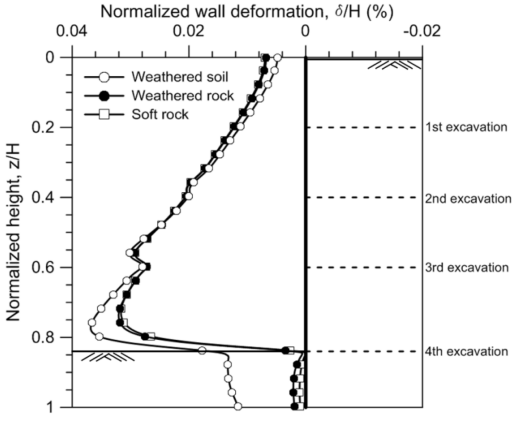

(b) Shaft deformation

Figure 8. Effect of bearing layer: (a) Lateral earth pressure distribution, (b) Shaft deformation.

show smaller lateral earth pressure and deformation for the embedded shaft compared to the floating shaft.

4.3 *Effect of shaft elastic modulus*

The effect of the shaft-soil stiffness, investigated by changing the elastic modulus of shaft, is shown in Fig. 9. As expected, lateral earth pressure acting on the shaft and behavior of shaft is highly influenced by the different stiffness as the elastic modulus increase. When the elastic modulus of shaft increases, arching effect of soil decreases. Once the elastic modulus of the shaft becomes lager than 28,000 MPa, there would be no arching effect such that the behavior of vertical shaft is like a rigid retaining wall. As the elastic modulus of shaft increase, the difference between results of Rankine's theory and those of this study decrease and get near to the distribution of lateral earth pressure at rest (i.e. K_0 condition).

5 CONCLUSION

The main objective of this study was to investigate a lateral earth pressure acting on a vertical circular shaft embedded in weathered soil. For this, a series of centrifuge model test and FE analyses for vertical shaft were performed.

The centrifuge model test shows that more realistic distribution of lateral earth pressure acting on a vertical circular shaft which is not linear with increasing excavation depth. Consequently, a commonly used theoretical method like the Rankine's equation for calculating the lateral pressure can substantially overestimate the lateral pressure in real situations.

Numerical analyses have been carried out for a wide variation of influence factors for lateral earth pressure acting on the vertical shaft. Numerical analyses showed the good agreement with the experimental measurements. Therefore, it could be said that the FE modeling techniques described in this study can effectively consider the soil arching effect.

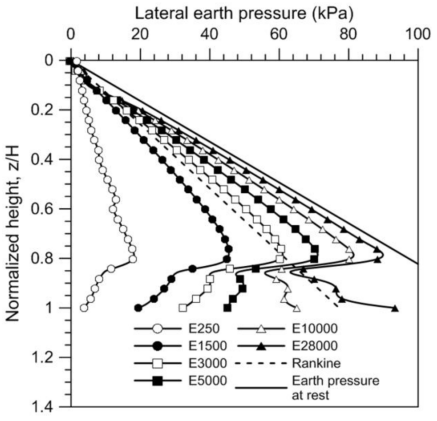

(a) Lateral earth pressure distribution

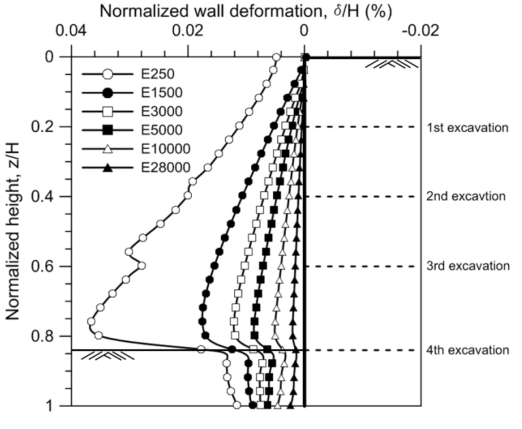

(b) Shaft deformation

Figure 9. Effect of shaft diameter: (a) Lateral earth pressure distribution, (b) Shaft deformation.

Based on the parametric study, it is found that the soil arching effect acting on the vertical circular shaft is significantly dependent on the following factors: the shaft diameter (D), the bearing layer and the elastic modulus of shaft (E). And it is also found that the arching effect is more significant for flexible vertical shaft than for rigid vertical shaft.

ACKNOWLEDGEMENTS

This work was supported by the National Research Foundation of Korea (NRF) grant funded by the Korea government (MSIP) (No. 2011-0030040).

REFERENCES

Handy, R. I., 1983. The arch in soil arching. *J. of Geotech. Eng., ASCE,* Vol. 111, No. 3, 302–318.

Harrop-Williams, K. O., 1989. Geostatic wall pressures. *J. Geotech. Engng, ASCE* 115, No. 9, 1321–1325.

Janssen, H. A., 1895. Versuche über getreidedruck in silozellen. Zeitschrift, *Verein Deutscher Ingenieure* 39, 1045–1049 (partial English translation in Proc. Inst. Civ. Engrs, 1986, 553.

Kim, K.Y., Lee, D.S., Cho, J.Y. & Jeong, S.S., 2013. The effect of arching pressure on a vertical circular shaft. *Tunelling and Underground space Technology*, Vol. 37, 10–21.

Liang, R. & Zeng, S., 2002. Numerical study of soil arching mechanism in drilled shafts for slope stabilization. *Soils and Foundations*., 42(2), 83–92.

Nakai, T., Xu, L. & Yamazaki, H., 1997. 3D and 2D model tests and numerical analyses of settlements and earth pressures due to tunnel excavation. *Soils and Foundations* 37 (3), 31–41.

Paik, K. H. & Salgado, R. 2003. Estimation of active earth pressure against rigid retaining walls considering arching effects. *Geotechnique*, Vol. 53, No. 7, pp. 643–653.

Spangler, M. G. & Handy, R. L., 1984. *Soil engineering*, New York: Harper & Row.

Tatiana T. & Mohamed A. M., 2010. Comparative evaluation of methods to determine the earth pressure distribution on cylindrical shaft: A review. *Tunnelling and Underground Space Technology* 25, 188–197.

Terzaghi, K., 1920. Old earth-pressure theories and new test results. *Eng. News-Record* 85 (13), 632–637.

Wang, Y. Z., 2000. Distribution of earth pressure on a retaining wall. *Geotechnique*, Vol. 50, No. 1, 85–88.

Wang, W.L. & Yen, B.C., 1973. Soil arching in slopes. *Journal of the Geotechnical Engineering, ASCE* 100 (1), 61–78.

Wong, R.C.K. & Kaiser, P. K. (1988), "Design and performance evaluation of vertical shaft: rational shaft design method and verification of design method", *Can. Geotech. J.*, Vol. 25, pp. 320–337.